JOURNAL OF MATERIALS SCIENCE 24 (1989) 247–251

Kinetic model for the mechanical properties of polymer glasses

YVES TERMONIA, DAVID J. WALSH
Central Research and Development, Experimental Station, E.I. du Pont de Nemours, Inc., Wilmington, Delaware 19880-0356, USA

The deformation behaviour and the mechanical properties of polymer glasses are studied with the help of a kinetic model introduced previously. The model, which is based on the Eyring chemical activation rate theory, takes into account the role of the strong attractive forces between macromolecular chains as well as chain slippage through entanglements. Application to poly(methyl methacrylate) has allowed us to calculate the yield stress, craze length and fracture toughness and their dependence on testing conditions. The model also clearly illustrates the transition from crazing to shear yielding in polymer glasses as the density of entanglements is increased.

1. Introduction

The fracture of polymer glasses is a very complex problem of great technological interest. Depending on the molecular weight, temperature, rate of deformation and other testing conditions, these materials may deform through shearing, craze formation or a combination of both. The molecular processes controlling these various modes of deformation are, however, not very well understood.

Several models have been proposed to describe the deformation behaviour of polymer glasses. The theories of Gent [1] and of Argon and Hannoosh [2] assume that crazing is formed by cavitation under hydrostatic tension in the polymer. Equations for describing the stress–strain relationships in polymer glasses have been proposed by Haward and Thackray [3] and Brown and Windle [4]. A finite-element analysis of craze deformation, assuming linear elastic behaviour, has been proposed by Bevan [5]. All these approaches, however, provide only a phenomenological or static representation of the deformation behaviour and they neglect the importance of the molecular weight and the entanglement network in polymer glasses. Recent studies [6–8], however, have demonstrated the profound effect of entanglements upon the mechanical properties of glassy polymers.

In a recent series of publications [9, 10] we have developed a new comprehensive, kinetic model for the study of the effect of molecular weight and entanglement density on the stress–strain curves and deformation behaviour of flexible polymers. In this approach, the polymer is represented by a loose entanglement network whose molecular chains are also tied together through numerous attractive bonds which provide the initial stiffness of the material. The model is extended here to a detailed study of the morphological changes occurring upon tensile deformation of glassy polymers. The effects of molecular weight and temperature on the toughness of these materials are also investigated.

2. Model

In the model (Fig. 1a), the polymer glass is represented by a dense array of entangled macromolecules which have a random coil configuration [11]. The heavy black circles represent entanglement points whereas the dotted lines denote the strong intermolecular interactions between molecules. These interactions provide the initial stiffness to the material [12]. For the purpose of convenience, our calculations are based on the more schematic representation given in Fig. 1b in which the heavy solid lines now denote chain vectors between entanglements, chain ends being indicated by broken solid lines. Individual attractive bonds have been also replaced by "overall" bonds (dotted lines) joining each entanglement point to its neighbours.

We start with a regular array of entanglements, as depicted in Fig. 1b. This array is filled in with macromolecular chains having a prescribed molecular weight distribution. This is performed using a step-by-step construction described elsewhere [9, 10, 13, 14]. The network of chains is then deformed along the y axis at a constant temperature and strain rate $\dot{\varepsilon}$. Upon tensile deformation, the following processes are allowed for in the model.

2.1. Breakage of the intermolecular attractions between chains

This bond breaking occurs in the early stages of the deformation process at strain values lower than 2%. The process is performed according to the kinetic theory of fracture [15], i.e. at a rate

$$\nu = \tau \exp\left[-(U - \beta\sigma)/kT\right] \quad (1)$$

In Equation 1, τ is the thermal vibration frequency; U and β are, respectively, the activation energy and

0022–2461/89 $03.00 + .12

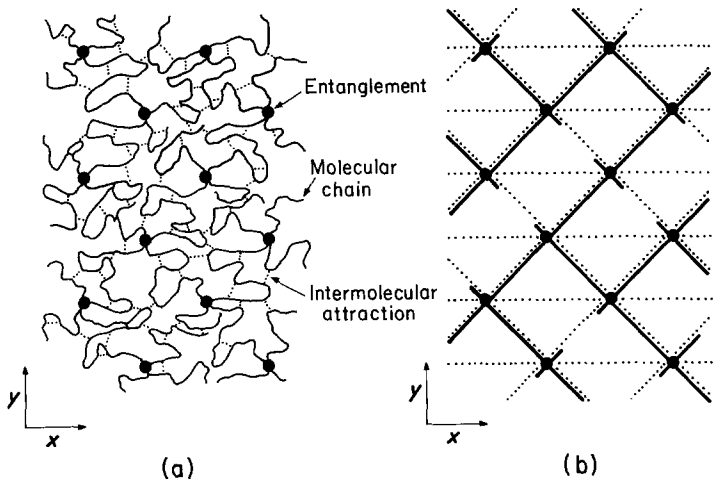

Figure 1 (a) Network representation of a polymer glass. The heavy black circles represent entanglement points, whereas the dotted lines denote the attractive forces between chains. (b) More schematic representation of the network in (a). The heavy solid lines denote chain vectors between entanglements, chain ends are indicated by broken solid lines. Individual attractive bonds have also been replaced by "overall" bonds (dotted lines) joining each entanglement point to its neighbours.

volume. σ is the local stress $\sigma = K\varepsilon$, where ε is the local strain and K the elastic constant for the attractive bond. These bond breakings lead to a release of the underlying chain strands which are now to support the external load. These chains, now free of intermolecular attractions, enter a rubbery state (see Equation 2 later) and start to extend between entanglements. As their stress increases, slippage of chain strands through entanglements sets in (Process 2 below).

2.2. Slippage of chains through entanglements

We assume that this occurs at a rate having the same functional form as Equation 1 but with different values for the activation energy U and activation volume β. Now σ represents the difference in stress in the two strands of a chain separated by an entanglement. According to the classical theory of rubber elasticity [16], the stress on a chain strand having a vector length r is

$$\sigma = \alpha \mathscr{L}^{-1}(r/nl) \qquad (2)$$

where n is the number of statistical chain segments and l is their length. $\mathscr{L}^{-1}$ is the inverse Langevin function and $\alpha = (n^{1/2}/3)K'$ where K' is the elastic modulus of the polymer in the rubbery region. In accordance with experimental data for flow in paraffins [16], we assume that the chain length capable of coordinated movement at a rate given by Equation 1 is of the order of 1 to 2 statistical segments. If slippage of chains through entanglements is too slow, i.e. at low temperatures or high strain rates, chain strands between entanglements will reach maximum extension and break (Process 3 below).

2.3. Breakage of chain strands at maximum elongation

This process occurs when the draw ratio for a chain strand exceeds $n^{1/2}$ where n is the number of statistical segments for that strand.

The above three processes are performed with the help of a Monte Carlo procedure [9, 10, 17] which, at regular short time intervals Δt, also relaxes the entanglement network to its minimum energy configuration. This is performed using a series of fast computer algorithms [17] which steadily reduce the net residual force acting on each entanglement. That relaxation procedure leads to displacements of the nodes along the tensile y axis. After that step, the sample is further strained by a small constant amount equal to $\dot{\varepsilon}\Delta t$. The Monte Carlo processes of attractive bond breaking, chain slippage and fracture are then restarted for another time interval Δt, and so on until the sample breaks.

Application of the above model to tensile deformation of poly(methyl methacrylate) (PMMA) was done using the following parameter values:

2.3.1. Attractive bond breaking

Values for the activation energy and volume are difficult to determine experimentally. We took $U = 25\,\text{kcal mol}^{-1}$ ($105\,\text{kJ mol}^{-1}$) $\beta = (0.82\,\text{nm})^3$*. These values were chosen in order to give a 2 to 3% strain at the yield point, together with a yield stress of around 80 MPa at room temperature [12]. The initial Young's modulus $K = 3\,\text{GPa}$.

2.3.2. Chain slippage

The molecular weight between entanglements $M_e = 4700$ [18] and the number n of statistical segments per chain strand equals 7, which leads to a maximum draw ratio $\lambda_{max} = 7^{1/2} = 2.6$ [19]. The modulus of PMMA in the rubbery regime, K', is about 2.75 MPa [20, 21]. We chose $U = 19\,\text{kcal mol}^{-1}$ ($80\,\text{kJ mol}^{-1}$) with $\beta = (0.6\,\text{nm})^3$ [9, 10]. The latter value is of the order of magnitude of a statistical chain segment.

3. Results and discussion

The model described above has been used to study the factors controlling the deformation behaviour of PMMA samples in tension.

Fig. 2 shows the calculated dependence of the yield stress on the rate of deformation at two different temperatures. Our stress values (open circles) are for a monodisperse PMMA with $M = 165\,000$. The results indicate an important decrease of the yield stress with a decrease in the rate of deformation. Our results are in reasonably good quantitative agreement with experimental data reported by Haward [22]. That

*These values are not for single bonds but for "overall" effective bonds linking every entanglement point to its neighbours [9, 10].

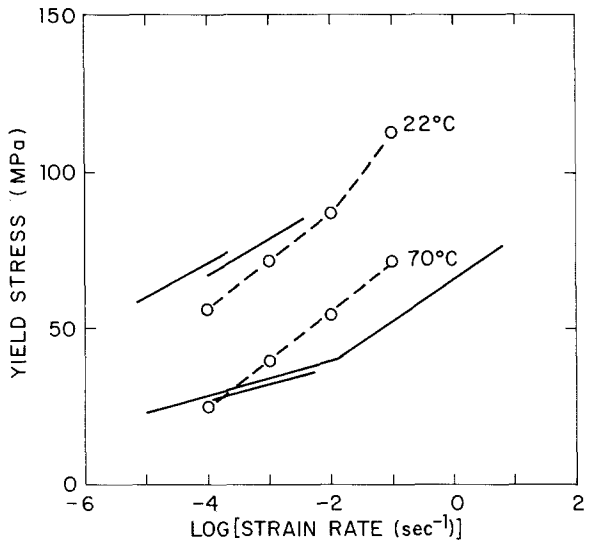

Figure 2 Dependence of the yield stress of PMMA on the rate of deformation at two different temperatures. Open circles are values calculated with the help of the model for a monodisperse polymer with $M = 165\,000$. Continuous lines denote experimental data reported by Haward [22].

agreement leads to strong support to our choice of values for the model's parameters.

We now turn to a detailed study of the deformation behaviour of notched PMMA samples in tension. Fig. 3a shows a typical notched specimen prior to deformation. The initial notch was obtained by breaking attractive bonds and molecular chain strands in the centre of the undeformed specimen within a small sphere having a diameter equal to 3% of the total sample width. Fig. 3b shows a typical deformation scheme obtained for monodisperse PMMA with $M = 165\,000$ at 22° C. The figure shows the presence of a very thin sheet of deformed polymer extending transversally from the initial central notch. That so-called craze structure is made of extended polymer fibrils separated by voids. Further investigation shows that these fibrils (for the high molecular weight considered) have a local draw ratio around 2.4, quite close to the maximum value $7^{1/2}$, in good agreement with experimental observation [19]. The voids, on the other hand, are created through the rupture of fibrils and retraction of their broken molecular chains. As the sample in Fig. 3b is further deformed, some of the fibrils will grow by drawing new polymer from the craze interface (craze thickening). Most of the fibrils, however, will progressively weaken either through disentanglement of chain strands or through breakage of chains at maximum extension. This leads to an enlargement of the voids, starting with those closest to the original notch (Fig. 3c). In this way, the overall craze grows weaker and weaker leading ultimately to catastrophic failure of the sample.

Fig. 3d shows the mode of deformation obtained for a glass, like poly(phenylene oxide), having a much larger density of entanglements. That change was obtained by tripling our initial value for the rubbery modulus K' (see Equation 2), which is proportional to the density of entanglements [16]. Comparing Figs 3b and 3d, which were obtained for the same value of the external strain, we observe a transition from a crazing to a shearing mode of deformation. The results for Fig. 3d do not show any chain breaking. Rather, upon increase of the external strain, the deformed zone thickens by drawing new polymer from the interface (Fig. 3e).

We now turn to calculate the craze length in PMMA with the help of the model. Since our simulations are limited by the memory and time available on the computer (IBM 3081D), the maximum sample width that can be reasonably handled on the computer is of the order of 1000 nm. That length is well below the experimentally observed craze length and the latter has therefore been estimated as follows. A series of short crazes of different lengths have been generated on the computer around small central cracks and strained at a constant rate of deformation. At some critical value of the external strain, these crazes reach

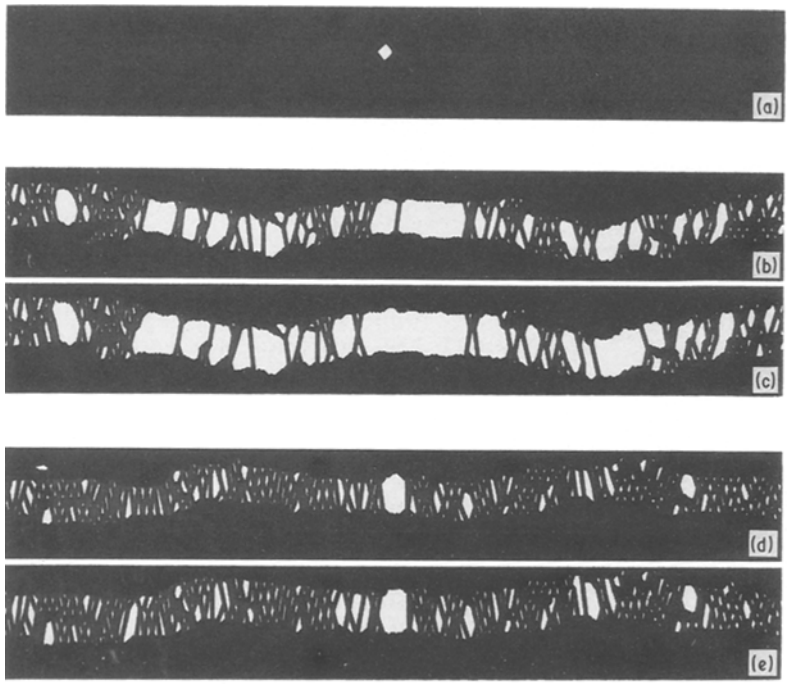

Figure 3 Deformation schemes obtained for notched PMMA samples in tension ($M = 165\,000$). (a) Before deformation; (b) PMMA at 15% external strain; (c) same specimen as in (b) but at 22.5% external strain; (d) polymer glass at 15% external strain and a density of entanglements three times higher than in (b) and (c); (e) same specimen as in (d) but at 22.5% external strain. Temperature was set equal to 22° C and rate of deformation $\dot{\varepsilon} = 0.01\ \text{sec}^{-1}$. The network has 50 nodes along the tensile y axis and 200 nodes in the transverse x direction. Assuming that the average distance between entanglements is of the order of 3 nm, the length of the samples along the horizontal x axis is of the order of 1 μm. The dark lines within the deformed regions in (b) to (e) denote extended chain strands.

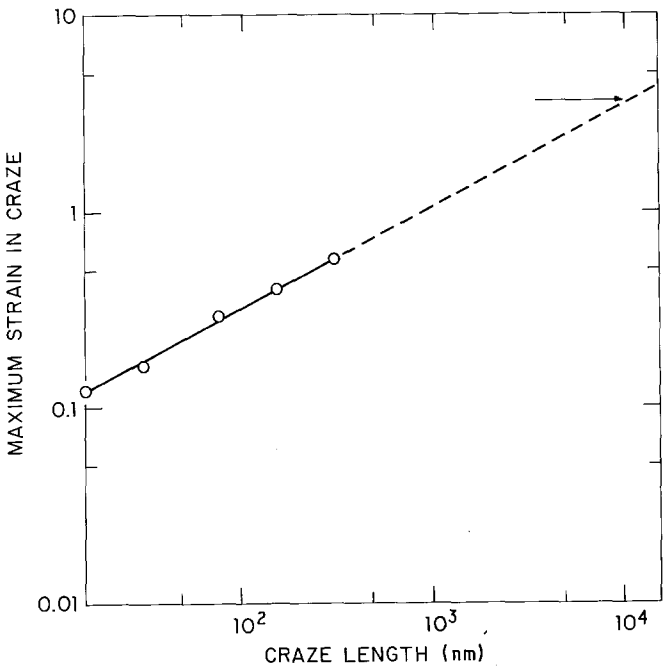

Figure 4 Dependence of the maximum engineering strain in craze on (half) the craze length. Networks of up to 400 × 100 nodes were used in the calculations. Temperature was set equal to 22° C and rate of deformation $\dot{\varepsilon} = 0.01\,\text{sec}^{-1}$.

the yield stress at their tip and start propagating. Values of the craze opening near the crack tip are then recorded and plotted against initial craze length (Fig. 4). We then make the assumption that the length of those propagating crazes will reach a stationary value when propagation at the craze tip is compensated by fibril breakage near the crack tip, i.e. when the craze opening reaches its maximum value. One shows easily that that maximum strain value is given by $\varepsilon_{max} = n^{1/2}3^{1/2} - 1 = 3.58$, where $n = 7$ is the number of statistical segments between entanglements, whereas the factor $3^{1/2}$ comes from geometrical considerations [9, 10]. Extrapolation of the results of Fig. 4 to $\varepsilon_{max} = 3.58$ leads to a calculated craze length around 12 μm, a value in good agreement with other estimations [23]. Note that our value probably constitutes a lower bound since its derivation neglects the possibility of slippage which would lead to an increase in ε_{max}.

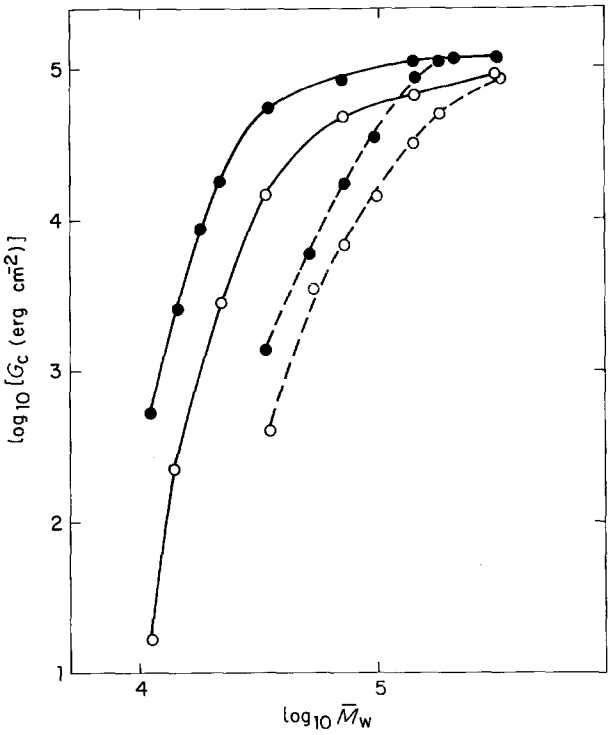

Figure 5 Calculated dependence of the fracture surface energy G_c on the (weight-average) molecular weight for PMMA at two different temperatures: (●) 22° C and (○) 60° C (1 erg cm^{-2} = 10^{-3} J m^{-2}). Continuous curves are for monodisperse samples; dashed curves are for polydisperse samples with $\overline{M_w}/\overline{M_n} = 3$ to 4. The rate of strain was set equal to 0.01 sec^{-1}. We took in Equation 4 $r_c = 100\,\mu$m, from experimental measurements reported by Kramer [25].

We now turn to present our results for the dependence of the fracture surface energy, G_c, on temperature and molecular weight, G_c has been calculated using

$$G_c = K_c^2/E \tag{3}$$

in which the fracture toughness K_c is obtained from the Dugdale plastic zone model [24]

$$K_c^2 = (8/\pi)r_c\sigma_c^2 \tag{4}$$

In Equation 4, r_c is the craze length, whereas σ_c is the maximum craze stress, as obtained with the help of our model.

Fig. 5 shows our calculated results for the dependence of G_c on (weight-average) molecular weight at two different temperatures. We took, in Equation 3, $E = 3$ GPa at 20° C and 2 GPa at 60° C, respectively. As a general result, the model shows a drop in G_c when $\overline{M_w}$ falls below 10^5. That observation is in accordance with a wealth of experimental data (see e.g. [26]). Our results for monodisperse samples (solid lines) also indicate a sharpe decrease in G_c with temperature for $\overline{M_w} < 40\,000$. That prediction is in good agreement with recent experimental observations [27]. Further investigation of our computer results shows that the decrease in G_c with temperature is due to chain slippage through entanglements, a process which is exacerbated at low molecular weights. We have also studied the effect of the molecular weight distribution on G_c. To this end, we have simulated on the computer the deformation behaviour of a series of PMMA glasses having a log-normal molecular weight distribution with $\overline{M_w}/\overline{M_n} = 3$ to 4. Our G_c values for these

polydisperse samples are presented in Fig. 5 (dashed lines). The results show a sharp decrease in toughness with polydispersity. Our G_c values become independent of polydispersity only for (weight-average) molecular weights higher than 200 000.

References

1. A. N. GENT, *J. Mater. Sci.* **5** (1970) 925.
2. A. S. ARGON and J. G. HANNOOSH, *Phil. Mag.* **36** (1977) 795.
3. R. N. R. N. HAWARD and G. THACKRAY, *Proc. R. Soc.* **A302** (1968) 453.
4. D. J. BROWN and A. H. WINDLE, *J. Mater. Sci.* **19** (1984) 2039.
5. L. BEVAN, *J. Polym. Sci., Polym. Phys.* **19** (1981) 1759.
6. R. P. KUSY and D. T. TURNER, *Polymer* **15** (1974) 394.
7. B. H. BERSTED, *J. Appl. Polym. Sci.* **24** (1979) 37.
8. A. M. DONALD and E. J. KRAMER, *Polymer* **23** (1982) 461.
9. Y. TERMONIA and P. SMITH, *Marcomolecules* **20** (1987) 835.
10. *Idem, ibid.* **21** (1988) 2184.
11. R. N. HAWARD, "The Physics of Glassy Polymers" (Applied Science, London, 1973).
12. A. S. ARGON and M. I. BESSONOV, *Polym. Eng. Sci.* **17** (1977) 174.
13. H. MEIROVITCH, *J. Phys.* **A15** (1982) L735.
14. *Idem J. Chem. Phys.* **79** (1983) 502.
15. S. GLASSTONE, K. J. LAIDLER and H. EYRING, "The Theory of Rate Processes" (McGraw-Hill, New York, 1941).
16. L. R. G. TRELOAR, "The Physics of Rubber Elasticity", 2nd Edn (Clarendon, Oxford, 1958).
17. Y. TERMONIA, P. MEAKIN and P. SMITH, *Macromolecules* **18** (1985) 2246.
18. J. D. FERRY, "Viscoelastic Properties of Polymers" (Wiley, New York, 1980) p. 374.
19. A. M. DONALD and E. J. KRAMER, *J. Polym. Sci.* **20** (1982) 899.
20. J. R. McLOUGHLIN and A. V. TOBOLSKY, *J. Colloid Sci.* **7** (1952) 555.
21. D. G. GILBERT, M. F. ASHBY and P. W. R. BEAUMONT, *J. Mater. Sci.* **21** (1986) 3194.
22. R. N. HAWARD, "The Physics of Glassy Polymers" (Applied Science, London, 1973) p. 296.
23. G. P. MARSHALL, L. H. COUTTS and J. G. WILLIAMS, *J. Mater. Sci.* **9** (1974) 1409.
24. J. R. RICE, in "Fracture, An Advanced Treatise", edited by H. Liebowitz (Academic, New York, 1968) Ch. 3.
25. E. J. KRAMER, *Adv. Polym. Sci.* **52** (1983) 1.
26. R. P. KUSY and D. T. TURNER, *Polymer* **17** (1976) 161.
27. D. WALSH and Y. TERMONIA, *Polyma Commun.* **29** (1988) 90.

Received 9 September 1987
and accepted 17 May 1988